# Downregulation of Membrane Trafficking Proteins and Lactate Conditioning Determine Loss of Dendritic Cell Function in Lung Cancer

Nicoletta Caronni, Francesca Simoncello, Francesca Stafetta, Corrado Guarnaccia, Juan Sebastian Ruiz-Moreno, Bastian Opitz, Thierry Galli, Véronique Proux-Gillardeaux, Federica Benvenuti

Published OnlineFirst January 23, 2018; DOI: 10.1158/0008-5472.CAN-17-1307

Tumor Biology and Immunology

Cancer Research

# Downregulation of Membrane Trafficking Proteins and Lactate Conditioning Determine Loss of Dendritic Cell Function in Lung Cancer

Nicoletta Caronni[1], Francesca Simoncello[1], Francesca Stafetta[1], Corrado Guarnaccia[1], Juan Sebastian Ruiz-Moreno[2], Bastian Opitz[2], Thierry Galli[3], Veronique Proux-Gillardeaux[3], and Federica Benvenuti[1]

## Abstract

Restoring antigen presentation for efficient and durable activation of tumor-specific CD8$^+$ T-cell responses is pivotal to immunotherapy, yet the mechanisms that cause subversion of dendritic cell (DC) functions are not entirely understood, limiting the development of targeted approaches. In this study, we show that *bona fide* DCs resident in lung tumor tissues or DCs exposed to factors derived from whole lung tumors become refractory to endosomal and cytosolic sensor stimulation and fail to secrete IL12 and IFNI. Tumor-conditioned DC exhibited downregulation of the SNARE VAMP3, a regulator of endosomes trafficking critical for cross-presentation of tumor antigens and DC-mediated tumor rejection. Dissection of cell-extrinsic suppressive pathways identified lactic acid in the tumor microenvironment as sufficient to inhibit type-I IFN downstream of TLR3 and STING. DC conditioning by lactate also impacted adaptive function, accelerating antigen degradation and impairing cross-presentation. Importantly, DCs conditioned by lactate failed to prime antitumor responses *in vivo*. These findings provide a new mechanistic viewpoint to the concept of DC suppression and hold potential for future therapeutic approaches.

**Significance:** These findings provide insight into the cell-intrinsic and cell-extrinsic mechanisms that cause loss of presentation of tumor-specific antigens in lung cancer tissues. *Cancer Res; 78(7); 1685–99. ©2018 AACR.*

## Introduction

Dendritic cells (DC) are the most potent and specialized class of antigen-presenting cells, essential to acquire and present tumor-associated antigens to T lymphocytes. Recent reports highlighted the key role of tissue-resident DCs in natural and therapy-induced tumor rejection (1–5). In early phases, DCs contribute to immune surveillance by sensing tumor-derived nucleic acid through the cytosolic sensors STING, and activation of the type-I IFN system (6, 7). In established tumors, DCs are required to prime T cells against tumor antigens and reactivate CTLs in tissues (4, 8). However, the tumor microenvironment (TME) targets DCs reducing the inherent capacity to recognize and activate tumor-specific CD8$^+$ T cells. This is caused by multiple overlapping mechanisms, including accumulation of DCs with poor antigen-presenting functions and immunosuppressive/tolerogenic properties (9–12) and direct suppression of fully differentiated cells *in situ*. For instance, IL10 produced by macrophages blocks IL12 production in models of breast cancer, whereas peroxidized lipids cause loss of cross-presentation in ovarian and EL-4 lymphoma cancer models (8, 13, 14). A lipid prostanoid, prostaglandin-E2, produced by overexpression of COX 1–2 enzymes in cancer cells, prevents inflammatory cytokine production and accumulation of CD103 cross-presenting DCs in mutant Braf melanoma models (3).

Despite these evidences, the molecular mechanisms that interfere with distinctive DCs cellular features are still poorly understood. DCs are unique among myeloid cells because they integrate sensing and firing of the innate response with antigen processing and cross-presentation of exogenous antigens to CD8$^+$ T cells. Molecularly, this is ensured by highly regulated and cell-specific expression of membrane-trafficking proteins that together orchestrate slow acidification in phagosome and export of antigens to the cytosol (15). In addition, membrane trafficking proteins are important for secretion of antitumoral cytokines, such as IL12 (16). Vesicular soluble N-ethylmaleimide sensitive proteins (v-SNARE) allow fusion of membranes across the biosynthetic and exocytic route (17). VAMP3 or cellubrevin is a V-SNARE that has been implicated in control of polarized recycling of the T-cell receptor and focal secretion of soluble mediators of inflammation in macrophages (18, 19). Whether and how membrane trafficking pathways are affected in tumor-exposed DCs has not been investigated.

A second gap-in knowledge is the limited understanding of immunosuppressive factors that target DCs in the TME. Increased lactate production is a hallmark of many cancer types that correlates to worsen prognosis, and whose detrimental effects are, in

[1]International Centre for Genetic Engineering and Biotechnology, Trieste, Italy. [2]Department of Internal Medicine/Infectious Diseases and Pulmonary Medicine, Charité University Medicine, Berlin, Germany. [3]Univ Paris Diderot, Sorbonne Paris Cité, Institut Jacques Monod, CNRS UMR 7592, Membrane Traffic in Health and Disease, INSERM ERL U950, Paris, France.

**Note:** Supplementary data for this article are available at Cancer Research Online (http://cancerres.aacrjournals.org/).

**Corresponding Author:** Benvenuti Federica, ICGEB, Padriciano 99, Trieste 34149, Italy. Phone: 39-040-375738; Fax: 39-040-3752226; E-mail: benvenuti@icgeb.org

**doi:** 10.1158/0008-5472.CAN-17-1307

Published OnlineFirst January 23, 2018; DOI: 10.1158/0008-5472.CAN-17-1307



part, mediated by suppression of immune cells (20–22). High lactate concentrations affect the function of T cells and NK cells, by inhibition of NFAT signaling and cytotoxic functions. In addition, lactate was shown to block differentiation of monocytes into DCs, DC activation, and monocyte metabolism and to promote accumulation of MDSC and M2 polarization of tumor-associated macrophages (22–25). Earlier studies suggest that lactate affects antigen presentation in DCs (26). However, the impact of lactate on IL12 and IFNI production, antigen cross-presentation, and priming of tumor-specific $CD8^+$ T cells by DCs has not been extensively explored.

In this study, we have investigated the origin of DCs dysfunction in a model of lung cancer, searching for intrinsic mechanisms and extrinsic factors determining suppression. We have identified downregulation of membrane-trafficking protein as an inherent modification occurring in DCs upon exposure to tumor-derived factors that limits antigen processing and presentation to $CD8^+$ T cells. In parallel, we have identified lactic acid as a key soluble factor that, independently of modulation of trafficking proteins, target DCs functions impairing innate response, antigen processing, and tumor rejection.

## Materials and Methods

### Mice

C57BL/6 mice were purchased from Harlan Laboratories and maintained in sterile isolators. $MyD88^{-/-}$ generated by S. Akira (27) were kindly provided by Anna Villa (Humanitas Research Hospital, Italy). $Asc^{-/-}$ mice (Genentech) were kindly provided by Sebastian Optiz (Charité – Universitätsmedizin). OT-I [C57BL/6-Tg(TcraTcrb)] originally generated by M. Bevan and F. Carbone were from The Jackson laboratory. OT-I on a Rag $1/2^{-/-}$ background were donated by Matteo Bellone (San Raffaele Scientific Institute, Milan, Italy). $VAMP3^{-/-}$ mice were originally from J.E. Pessin (Albert Einstein College of Medicine, New York, NY) and their genetic background was changed to C57BL/6 following >6 backcrosses. Animal care and treatment were conducted in conformity with institutional guidelines in compliance with national and international laws and policies (European Economic Community Council Directive 86/609; OJL 358; December 12, 1987). All experiments were performed in accordance with the Federation of European Laboratory Animal Science Association guidelines and protocols were approved by the Italian Ministry of Health (Aut. N.1155/2016-PR).

### Cell lines

The Lewis lung carcinoma cell line 3LL (LL2, LLC/1) has been purchased by the ATCC (CRL-1642) in October 2014. LLC-Thy1.1-OVA (3LL-OVA) was derived from LL2 by retroviral transduction with a pMIG retroviruses containing the following inserts: Thy1.1; OVA IRES Thy1.1 and kindly donated by Dr. Douglas Fearon (Cancer Research UK Cambridge Institute, Cambridge, United Kingdom) in April 2015. The lung adenocarcinoma cell line LG1233 was derived from lung tumors of C57BL/6 KP mice ($K\text{-}ras^{LSL\text{-}G12D/+}$;$p53^{fl/fl}$ mice) and was kindly provided by Dr. Tyler Jacks (Massachusetts Institute of Technology, Cambridge, MA) in July 2015. LG1233 was not authenticated. All cell lines were maintained in DMEM supplemented with 10% FBS and gentamicin (50 μg/mL) and routinely tested for *Mycoplasma* contamination. All cell lines were expanded to passage 3 and stored in aliquots in liquid nitrogen; to induce tumors, cells were cultured less than five passages.

### Tumor conditioned medium

Tumor conditioned medium was obtained as described previously (14).

In brief, $0.5 \times 10^6$ 3LL or LG, were injected subcutaneously into the right flank of C57BL/6 mice. Mice were sacrificed and tumor collected 21 days after injection. Tumor masses were cut in small pieces and incubated with Collagenase type 2 (265 U/mL; Worthington) and DNase (250 U/mL; Thermo Scientific) at 37°C for 1 hour. After red blood lysis and dead cell exclusions, using the Dead Cell Removal Kit (Miltenyi Biotec), cells were plated overnight at the concentration of $10^7$ cells/mL and the cell-free supernatant collected. For some experiments, 3LL TCM was boiled for 10 minutes at 95°C, centrifuged 5′ at 14,000 rpm, and the protein-free supernatant was used for DC conditioning (3LL boiled). Fractionation of TCM has been performed by using Amicon Ultra-0.5 Centrifugal Filter Unit (Ultracel 3 KDa, Millipore) and centrifuging the supernatant at 5,000 rpm. The supernatant fraction >3 kDa remained above the filter and the <3 kDa passed through to the bottom chamber. Both fractions were resuspended in DMEM to the prefiltration volume.

Where indicated, TCM has been obtained by culturing 3LL cells in 24-well plate at the concentration of $3 \times 10^5$/mL, in the presence of LDHA inhibitor, 5 μmol/L (GSK 2837808A, Tocris Bioscience) or its vehicle DMSO. Supernatants were collected after 48 hours of culture.

The concentration of lactic acid in the obtained TCM was measured by using the Lactate Colorimetric Assay Kit II (BioVision).

### Lung orthotopic tumor model

To establish lung orthotopic tumors, 3LL cells were harvested and wash three times with cold PBS and mixed at a 1:1 ratio with Geltre LDEV-Free Reduced Growth Factor Basement Membrane Matrix (Gibco). A total of $1 \times 10^4$ 3LL cells in a final volume of 20 μL was injected into the left lung lobe by intercostal injection at the median axillary line of C57BL/6 mice. Tumors were collected at day 21 or 28 after engraftment.

### Lung tumor DC isolation

Tumor-bearing lungs were harvested after PBS lung circulatory perfusion, mechanically cut into small pieces, and digested with Collagenase type 2 (265 U/mL; Worthington) and DNase (250 U/mL; Thermo scientific) at 37°C for 30 minutes. Collagenase was then stopped by EDTA 10 mmol/L and the cell suspension was filtered using 40-μm cell strainer (Corning). $CD11c^+$ lung cells were separated by immunomagnetic sorting using CD11c microbeads (Miltenyi Biotec) following the manufacturer's instructions. DCs were purified by FACS sorting with FACS Aria II (BD Biosciences), using the gating strategy shown in Fig. 1A, after $CD11c^+$ cells staining in PBS + 2% FBS with the following antibodies: CD11c-A647 (N418), and CD24-PEDazzle594 (M1/69) purchased from eBioscience and SiglecF-BB515 (E50-2440) and MHCII-BV711 (M5/114.15.2) from BD Biosciences. For gene expression analysis, up to 30,000 cells were sorted directly into 350 μL RLT buffer (Qiagen). For *ex vivo* DC stimulation, $1 \times 10^4$ cells were plated in U-bottom 96-well plate and stimulated for 3 hours with CpG-B (1 μg/mL; ODN 1668; InvivoGen) PolyI:C (10 μg/mL; InvivoGen) or LPS (1 μg/mL;

Published OnlineFirst January 23, 2018; DOI: 10.1158/0008-5472.CAN-17-1307



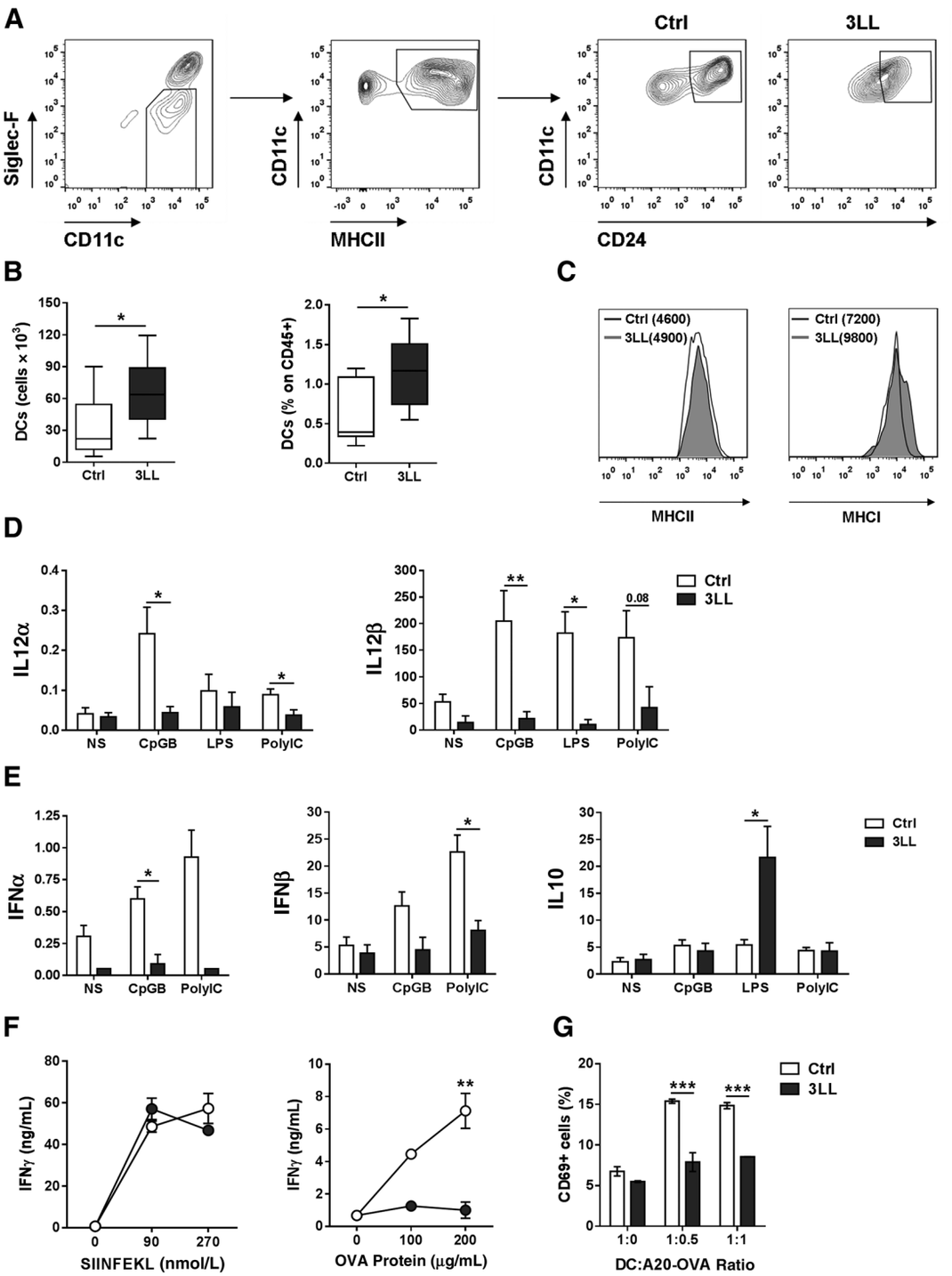


**Figure 1.**

Suppression of tissue-resident lung DCs in tumor-bearing host. **A,** Gating strategy for the identification of DCs in lungs of healthy or 3LL othrotopic tumor-bearing mice at day 28 post-implantation. **B,** Absolute numbers (left) and percentages (right) of DCs in control and tumor-bearing mice. Data represent the mean ± SEM of $n \geq 10$ mice per group. **C,** Representative histogram of MHCII and MHCI expression by control or T-DCs. **D** and **E,** Relative expression of *IL12α, IL12β, IFNα, IFNβ,* and *IL10* in control and tumor-derived FACS-sorted DCs after 3 hours of *ex vivo* stimulation with the indicated agonists. Data were normalized on Gapdh and are presented as mean ± SEM of five independent experiments. **F** and **G,** T-cell activation assay. Control and 3LL-derived DCs were pulsed with OVA class I peptide (left), OVA protein (right), or apoptotic A20-OVA cells at different ratios (**G**) and coincubated with $CD8^+$ OT-I. IFNγ was quantified by ELISA upon 48 hours of coculture and percentage of $CD69^+$ cells was analyzed by FACS after 16 hours of coculture. Data are pooled from individual mice ($n = 5$). Significance was determined by an unpaired *t* test or two-way ANOVA; *, $P \leq 0.05$; **, $P \leq 0.01$; ***, $P \leq 0.001$. NS, not stimulated.

Published OnlineFirst January 23, 2018; DOI: 10.1158/0008-5472.CAN-17-1307



InvivoGen) and then lysed in RLT buffer (Qiagen) for gene expression quantification. For *ex vivo* T-cell activation assay, $1 \times 10^4$ cells/well were plated in U-bottom 96-well plate, stimulated with polyI:C (1 μg/mL) and pulsed with class I OVA peptide, OVA protein or UV-irradiated A20-OVA cells at indicated doses. A20-OVA were generated by transducing A20 with a lentiviral vector encoding Ii-OVA (kindly provided by David Murrugarren, CIB, Navarra). To induce apoptosis cells were exposed to UV-C irradiation for 30 seconds and further cultured for 8–12 hours in PBS. After 3-hour stimulation, cells were washed twice in PBS and coincubated with $1 \times 10^5$ $CD8^+$ isolated OT-I T cells. IFNγ was quantified by ELISA upon 48 hours of coculture, whereas the percentage of $CD69^+$ cells was assessed after 16 hours of coculture by FACS.

### FL-DCs

Mouse FL-DCs were generated from bone marrow of C57BL/6 wt, MyD88$^{-/-}$, Asc$^{-/-}$, or VAMP3$^{-/-}$ mice. Bone marrow cells were cultured at the concentration of $1.5 \times 10^6$ cells/mL in Nunc nontreated 6-well plates (Thermo Scientific) for 7 days using Iscove's modified Dulbecco's medium supplemented with 10% FBS, 50 μmol/L 2-Mercaptoethanol (Gibco), 0.2% of primocin (InvivoGen), and 15% of Flt3L-containing supernatant, produced from an SP2/0 transfected cell line that secretes murine recombinant Flt3L. At day 7 of culture, cells were harvested and conventional DCs were depleted of $B220^+$ cells (Miltenyi Biotec kit, CD45R; B220). Depending on the experiment, cells were conditioned for 3 or 24 hours with TCM at the ratio of 1:1 with medium or lactic acid 10 mmol/L [L-(+)-Lactic acid, Sigma]. Cells were lysed in TRIzol after 3 hours of conditioning for proinflammatory cytokine gene quantification or after 24 hours of TCM for SNARE expression quantification. For stimulation experiments, after 24 hours of conditioning, cells were harvested, washed, and plated $2 \times 10^6$ cells/mL in 96-well plates at 37°C with CpG-B (1 μg/mL; ODN 1668 InvivoGen), polyI:C (10 μg/mL; InvivoGen), LPS (1 μg/mL; InvivoGen), or DMXAA (25 μg/mL; InvivoGen). Where indicated, DCs were conditioned with TCM in the presence of anti-IL-10R mAb (clone 1B1.3; 10 μg/mL; eBiosciences) and anti-TGFβ 1, 2, 3 antibody (clone 1D11; 10 μg/mL; R&D Systems). After overnight culture, cytokine concentrations in the supernatant were determine by ELISA.

### *In vitro* T-cell activation assay

FL-DCs were plated at $2 \times 10^4$ cells/well in U-bottom 96-well plate and conditioned for 2 hours with TCM (1:1) or lactic acid (10 mmol/L). Without washing the conditioned media, DCs were then stimulated with CpG-B (1 μg/mL) and polyI:C (1 μg/mL) and pulsed for 3 hours with OVA class I peptide (SIINFEKL), OVA protein, or UV-irradiated A20-OVA cells at indicated doses. After antigen feeding, $1.5 \times 10^5$ RagOT-I cells were added to DC-containing wells for 48 hours. IFNγ production was quantified by ELISA after 48 hours of coculture.

### pH-rodo

FL-DCs were conditioned with lactic acid (10–20 mmol/L) for 1 hour at the concentration of $2.5 \times 10^6$/mL. Cells were then washed and pulsed 15′ at 37°C with pHrodo Green Dextran (20 μg/mL; Thermo Scientific), washed twice with cold PBS and reincubating at 37°C. At the indicated time point (0-30-90′) cells were washed, incubated at 4°C and pHrodo fluorescence was analyzed by FACS.

### DQ BSA

FL-DCs were conditioned with lactic acid (10–20 mmol/L) for 1 hour at the concentration of $2.5 \times 10^6$/mL. After 45 minutes of conditioning, CpG-B (1 μg/mL) and polyI:C (1 μg/mL) were added to the cell suspensions for 15 minutes of stimulation. Cells were then washed and pulsed 15′ at 37°C with BSA medium, containing DQ Green BSA (5 μg/mL; Thermo Scientific) and A647-BSA (5 μg/mL; Molecular Probes). After BSA pulse, cells were washed twice with cold PBS, to remove aspecific-bounded BSA from the cell surface, and cells were incubated for 10 minutes at 37°C, then washed and fixed with PBS + 1% PFA. DQ-BSA lysosomal degradation was measured by flow cytometry as the percentage of $FITC/DQ\text{-}BSA^+$ cells, normalized on $A647^+$ cells.

### Phagocytosis assay

To assess phagocytosis, wt or VAMP3$^{-/-}$ DCs were incubated with fluorescent latex beads (Polyscience, 1 μm). Different amounts of a 1:50 dilution of the stock ($4.55 \times 10^{10}$ beads/mL) corresponding to a DC:beads ratio of 1:25, 1:50, 1:100, 1:200 were used. Values of uptake at 4°C were subtracted before plotting the data.

### Tumor/DC coinjection and *ex vivo* T-cell restimulation

Wt or VAMP3$^{-/-}$ DCs were stimulated for 30 minutes with CpG-B (1 μg/mL) and poly I:C (1 μg/mL), then resuspended in PBS at the concentration of $3 \times 10^6$/mL and coinjected subcutaneously in the right flank of shaved C57BL/6 mice with LLC-Thy1.1-OVA at the ratio of 1:1. After 14 days from tumor inoculation, spleen of tumor-bearing mice was harvested and disaggregated. Splenocytes were *ex vivo* restimulated with class I OVA peptide (2 μmol/L) for 5 hours, in the presence of BD-Golgi Stop (1:1,000; BD Biosciences). IFNγ production was measured by intracellular staining and flow cytometry analysis. Tumor growth was monitored every 2 days by calipers and tumor size was determined by the formula $(d_1 \times d_2^2)/2$.

### *In vivo* T-cell priming and tumor rejection

FLDCs were conditioned for 2 hours with lactic acid (10 mmol/L) and then stimulated for 3 hours with CpG-B (1 μg/mL) and polyI:C (1 μg/mL) and pulsed with class I OVA peptide (100 nmol/L) for 3 hours. Cells were then washed and injected $3 \times 10^5$ cells in the footpad of C57BL/6 mice, previously intravenously transferred with $1 \times 10^6$ RagOT-I. Blood and popliteal lymph nodes were collected 14 days after DC injection and restimulated *ex vivo* with class I OVA peptide (2 μmol/L) for 5 hours, in the presence of BD-Golgi Stop (1:1,000; BD Biosciences). IFNγ production was measured by intracellular staining and flow cytometry analysis.

For tumor rejection experiments, DCs were treated as described above, but injected subcutaneously in the right flank of C57BL/6 mice, which also received after 14 days $3 \times 10^5$ LLC-Thy1.1-OVA. Tumor growth was monitored every 2 days by calipers and tumor size was determined by the formula $(d_1 \times d_2^2)/2$.

### Flow cytometry

The following antibodies were obtained from BioLegend: CD11c-A647 (N418), CD45-PercPcy5.5 (30-F11), CD24-PEDazzle594 (M1/69), MHCII-APC/A488 (AF6-120.1), CD8-APC (53-6.7), TCR Vα5.2-PercPcy5.5 (B20.1), IFNγ-PE (XMG1.2) and CD69-PE (H1.2F3). From BD Biosciences, the following antibodies were purchased: CD86-PE (B7-2), TCR Vβ5.2-FITC (MR9-4).

Published OnlineFirst January 23, 2018; DOI: 10.1158/0008-5472.CAN-17-1307



MHCI-PE (AF6-88.5.5.3) was obtained from eBioscience. Viability was assessed by staining with the LIVE/DEAD Fixable Aqua Dead Cell Stain Kit (Life Technologies), Fixable Viability Dye eFluor 780 (eBioscience), or Annexin V/7AAD kit (Life Technologies).

For cell staining, FcR-binding sites were blocked by using αCD16/CD32 (93, Biolegend). Samples were then stained with specific antibodies in PBS + 1% BSA and fixed with PBS + 1% PFA. For intracellular staining, cells were stimulated with SIINFEKL 100 nmol/L 37°C for 5 hours, adding Golgi Stop (BD Biosciences) to allow accumulation of intracellular cytokines. After viability and surface marker staining, cells were fixed and permeabilized using Cytofix/Cytoperm solution (BD Biosciences) following the manufacturer's instructions, and then stained with anti-IFNγ. Flow data were acquired with a FACS Celesta (BD Biosciences) and analyzed with Diva software (BD Biosciences) or FlowJo software (Tree Star, Inc.).

### Real-time PCR

Total RNA was extracted from DCs with TRIzol reagent or using the RNeasy Micro Kit (Qiagen) according to the manufacturer's instruction. cDNA was synthesized using SuperscriptII reverse transcriptase (Invitrogen) or SuperScript VILO (Invitrogen). Real-time PCR for gene expression was performed using SsoFast EvaGreen Supermix (Bio-Rad) and specific primers listed in Supplementary Table S1.

### ELISA

IL12p70, IL10, and IFNγ were detected by ELISA Max Standard sets (Biolegend), following the manufacturer's instructions. IFNα in supernatant was measured by using rat monoclonal anti-mouse IFNα, clone RMMA-1 (pbl assay science) as capture antibody and rabbit polyclonal anti-mouse IFNα, rabbit Serum (pbl assay science) as detection antibody. Samples were then incubated with anti-rabbit IgG, HRP-linked antibody (Cell Signaling Technology), followed by TMB Substrate Solution (Sigma). Finally, the Stop Solution (HCl 1 mol/L) was added to the reaction and the absorbance was red at 450 nm with iMar Microplate Absorbance Reader (Bio-Rad).

### LC-MS

Duplicate samples were diluted 10x in acetonitrile/50 mmol/L NH4OAc pH4.5 (9:1). The same 4 samples (DMEM $C^+$, TCM 3LL boiled, TCM LG, TCM 3LL) were analyzed after a 5 mmol/L lactate spike to evaluate eventual matrix interferences; 5 μL of each sample was injected using a 3x full loop injection. The liquid chromatography was performed by hydrophilic interaction chromatography (HILIC) using a ZIC-HILIC column (2.1 × 150 mm, 3.5 μm, Merck Sequant). Mobile Phase A was 50 mmol/L NH4OAc, pH 4.5 and Mobile Phase B was acetonitrile, the separation was performed using a gradient from 90% B to 0% B in 18 min at 0.25 mL/min. The amaZonSL hyphenated mass spectrometer (Bruker Daltonics, Bremen, Germany) was operated in MRM in negative ion mode monitoring the m/z 89 (parent ion) to 43.1 (fragment ion) transition. Area integration analysis was performed using the Compass Data Analysis software (Bruker).

### Statistical analysis

Statistical significance was determined using an unpaired two-tailed Student *t* test, two-way ANOVA, one-way ANOVA, Kruskal–Wallis or Log-rank (Mantel-Cox) test as indicated. Survival in mouse experiments are reported as Kaplan–Meier curves and significance was determined by log-rank test. A *P* value of ≤0.05 was considered significant (*, $P \leq 0.05$; **, $P \leq 0.01$; ***, $P \leq 0.001$; ****, $P \leq 0.0001$).

## Results

### DCs conditioned by lung tumor microenvironment lose the capacity to produce inflammatory cytokines and to present antigens to T cells

We first set-up the model to compare tissue resident DCs isolated from lungs of healthy or tumor-bearing mice. To this aim, we injected orthotopically $1 \times 10^4$ 3LL (LLC/1) cells in the left lung lobe. Lesions were clearly visible starting at day 14 post-inoculation and lungs were harvested between day 21 and 28 to analyze the composition of the DCs compartment. We applied an accurate gating strategy to exclude alveolar macrophages and identify *bona fide* tissue resident lung DCs (Fig. 1A). Siglec-$F^-$/$CD11c^{high}$/MHC-$II^+$/$CD24^+$ cells were increased in frequency and absolute numbers in the tumor injected lobe, as compared with control lobes from healthy animals (Fig. 1B). Expression of MHC class-II was similar whereas MHC class-I was slightly enhanced on tumor-associated DCs (Fig. 1C). Next, we isolated lung-DCs by cell sorting to probe their capacity to respond to innate stimuli. Thus, cells were restimulated *ex vivo* and expression of cytokine genes was assessed by RT-PCR, as numbers were too few to allow protein detection. Control lung DCs induced transcription of both IL12 subunits and of the two type-I interferon species (IFNα and β) upon stimulation with agonists of TLR9, TLR4 and TLR3. In contrast, DCs isolated from lung tumors showed little or no proinflammatory gene induction and instead upregulated the production of the immune-suppressive cytokine IL10 (Fig. 1D and E). To assess antigen presentation, we incubated cell-sorted DCs with OVA MHC class-I peptide (SIINFEKL) or intact OVA protein and mixed them to OVA-specific transgenic $CD8^+$ T cells (OT-I). Presentation of peptide was equally efficient in control and tumor DCs. In contrast, the ability to cross-present OVA intact protein was largely lost in tumor derived DCs (Fig. 1F). Moreover, we generated an A20-OVA cell line (H-2Kd background), to assess cross-presentation of cell-associated antigens. When tumor conditioned DCs were incubated with apoptotic A20-OVA cells, they failed to activate OTI T cells, confirming loss of presentation of tumor-derived antigens by DCs in the tumor tissue (Fig. 1G).

Loss of innate and adaptive activities by tumor tissues DCs likely reflects multiple complex steps that are kinetically difficult to dissect. To address early events occurring in DCs upon exposure to tumor-derived factors, excluding confounding contributions by different activation and differentiation stages, we exposed *in vitro* Flt3L differentiated DC (FL-DCs) to tumor-derived factors (TCM, obtained by culturing dissociated tumor mass in medium). FL-DC exposed to 3LL TCM upregulated MHC-II, CD86 and MHC-I. We tested as well a second lung tumor cell line derived from $Kras^{G12D/+}$;$Trp53^{-/-}$, KP mice, referred to as LG (Fig. 2A and B; refs. 28, 29). Besides phenotypic maturation, 3LL and LG TCM triggered rapid induction of IL1β and IL6 transcripts in tumor-exposed DCs (Fig. 2C). Despite initial activation, 3LL TCM-conditioned DCs were refractory to produce bioactive IL12p70 or to secrete IFNα in response to CpG-B, LPS, polyI:C and agonist of the cytosolic sensor STING (DMXAA). Instead, TCM-treated DCs enhanced secretion of IL10 upon TLR4

Published OnlineFirst January 23, 2018; DOI: 10.1158/0008-5472.CAN-17-1307



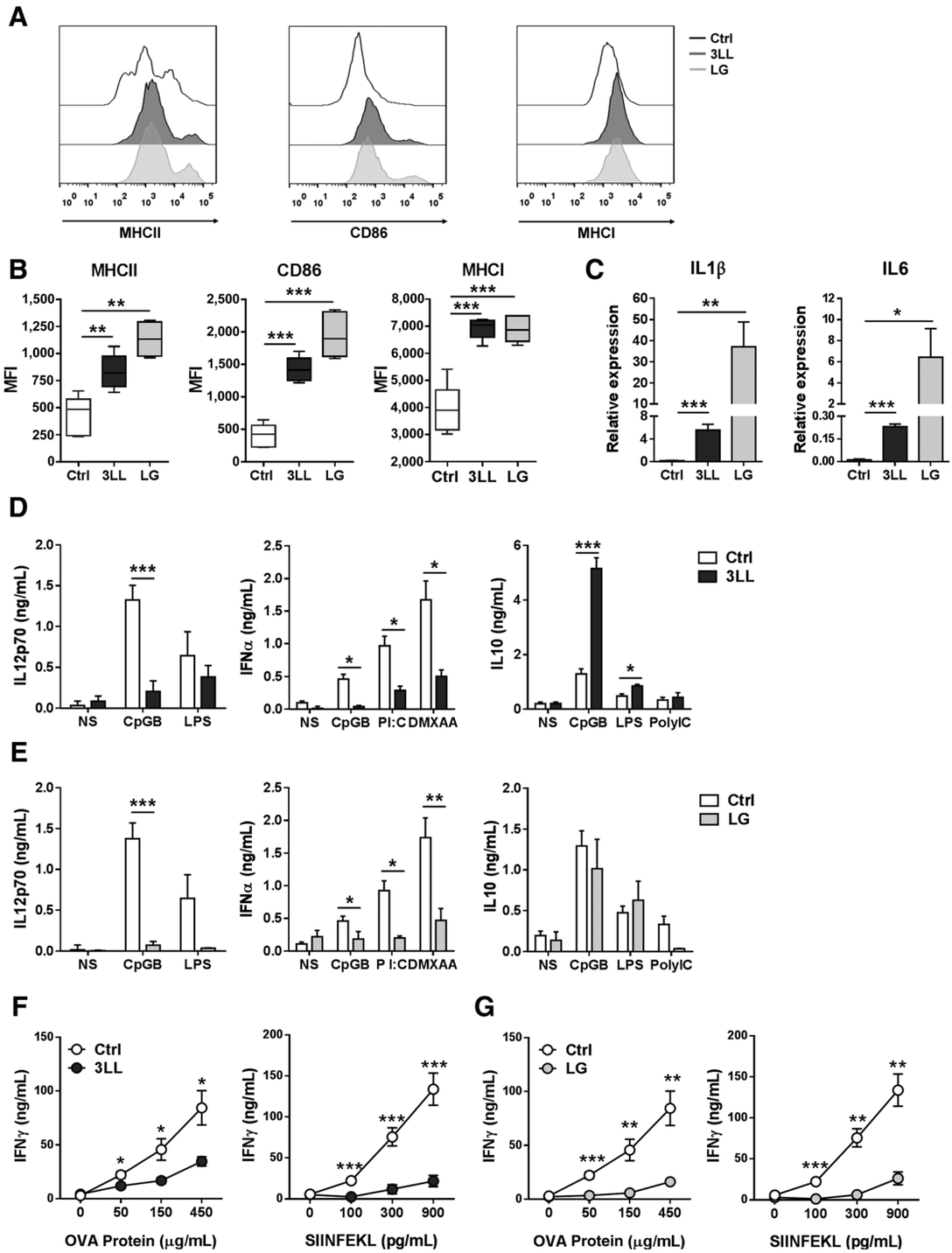


**Figure 2.**

Tumor-derived factors block cytokine production and CD8$^+$ T-cell activation in DCs. **A** and **B,** Representative histograms (**A**) and median fluorescence intensity (MFI; **B**) of MHCII, CD86, and MHCI expression by FL-DCs 24 hours after conditioning with 3LL or LG TCM. **C,** Relative expression of *IL1β* and *IL6* in control, 3LL-, and LG-conditioned DCs. Cells were harvested 3 hours after treatment with TCM (1:2). Data were normalized on Gapdh and are presented as mean ± SEM of six independent experiments. **D** and **E,** Cytokine suppression experiments. DCs were conditioned for 24 hours with TCM (1:2), washed and stimulated overnight with CpG-B (1 μg/mL), polyI:C (10 μg/mL), LPS (1 μg/mL), or DMXAA (25 μg/mL). Cytokine production was assessed by ELISA. Data are presented as mean ± SEM of eight independent experiments. **F** and **G,** *In vitro* T-cell activation assay. TCM-conditioned FL-DCs were pulsed with OVA class I peptide or OVA protein for 3 hours, followed by coincubation with Rag OT-I T cells for 48 hours. Bars show IFNγ levels measured by ELISA. Data represent the mean ± SEM of three independent experiments. Significance was determined by an unpaired *t* test; *, $P \leq 0.05$; **, $P \leq 0.01$; ***, $P \leq 0.001$. NS, not stimulated.

Published OnlineFirst January 23, 2018; DOI: 10.1158/0008-5472.CAN-17-1307



stimulation (Fig. 2D). A similar trend was found for the LG TCM, except for IL10 induction that remained unchanged upon TCM treatment (Fig. 2E). We next moved to assess the ability of DCs to activate T cells *in vitro*. FL-DCs loaded with peptide or intact OVA protein induced a dose-dependent production of IFNγ by OVA-specific $CD8^+$ T cells. In contrast, FL-DC conditioned by 3LL or LG TCM failed to activate T cells efficiently, both in the case of peptide and intact protein (Fig. 2F and G). The inability to present peptide, despite elevated expression of maturation markers, may depend on lack of costimulatory cytokines or failure to interact with T cells (30, 31). In conclusion, DCs conditioned by lung cancer TME *in vitro* and *in vivo*, show loss of responsiveness to agonist of innate sensors and are unable to activate antigen-specific T cells.

### Loss of membrane trafficking protein leads to defective cross-presentation in tumor-exposed DCs

On the basis of the above findings, we reasoned that loss of antigen presentation in tumor-exposed DCs may depend on alteration of the finely tuned trafficking machinery that orchestrate antigen handling. Proteins of the SNARE and Rab family are important regulator of antigen-processing and cytokine secretion in DCs (16, 32–34). The importance of these pathways is undescored by SNARE downregulation by viruses as a mechanism of escape (35, 36). We quantified transcripts for 3 proteins representative of different steps along the endocytic pathway. VAMP3 marks recycling endosomes (17, 19, 37) and has been implicated in secretion of TNF by macrophages. Stx6 is involved in post-Golgi trafficking (38) and Rab27 is associated to the endo-lysosomes and cross-presentation in DCs (32). Interestingly, transcription of the 3 proteins was decreased in DCs isolated from early 3LL tumor tissues and strongly inhibited in DCs isolated from advanced tumors (Fig. 3A). Similarly, incubation of FL-DCs with TCM of 3LL or LG tumors *in vitro* caused strong down-regulation of VAMP3, Rab27 and Stx6 (Fig. 3B and Supplementary Fig. S1A). Thus, exposure to tumor-derived factors both *in vivo* and *in vitro* affects the expression of trafficking-related genes. As VAMP3 was the most consistently downregulated transcript, we examined the functional relevance of its loss in DCs. Cells differentiated from VAMP3 null mice (39) show no defect in phenotypic maturation (Supplementary Fig. S1B) and a slight reduction in IL12 secretion, whereas IFNI levels were unchanged (Supplementary Fig. S1C and S1D). Phagocytosis of fluorescent latex beads was not affected by VAMP3 deficiency (Supplementary Fig. S1E). Despite intact engulfment of particles, presentation of cells associated OVA was largely diminished in the absence of VAMP3 (Fig. 3C), whereas cross-presentation of soluble OVA protein or peptide were intact. Thus, these data suggest that VAMP3 is required to process cell associated antigens downstream of apoptotic cell uptake. To evaluate the impact of VAMP3 deficiency on antitumor immune responses *in vivo*, we inoculated mice with 3LL-OVA tumor cells alone or mixed with DCs. Coinjection of tumor cells with wt DCs induced IFNγ production by antigen specific $CD8^+$ T cells and strongly inhibited tumor growth. In contrast, coadministration of tumor cells with $VAMP3^{-/-}$ DCs induced only a weak response and was unable to block tumor progression (Fig. 3D and E). Therefore, diminished expression of VAMP3 in tumor-exposed DCs affects the inherent capacity to cross-present tumor-associated antigen and to initiate antitumor responses.

### DCs suppression does not depend on innate sensors nor on blockade of IL10 or TGFβ

We next asked what cell extrinsic factors cause suppression of cytokine production and antigen presentation in our model. A recent report showed that versican contained in the supernatant of 3LL cells induces tolerogenic DCs via TLR2 dependent activation (40). To understand whether a similar mechanism accounts for loss of IL12, IFNI, and T-cell priming we tested cells derived from $MyD88^{-/-}$ mice. Early transcription of Il1b and Il6 was similarly induced by the TCM in wt and $MyD88^{-/-}$ cells (Supplementary Fig. S2A). Cytokine production upon restimulation with CpG-B was blunted in MyD88 null cells as expected, whereas IFNI responses to polyI:C and DMXAA were normal (Supplementary Fig. S2B). Interestingly, exposure to the TCM, abolished IFNI responses and T-cell priming in $MyD88^{-/-}$ DCs (Fig. 4A and B and Supplementary Fig. S2C). The early induction of IL1β, suggested a possible role of inflammasome activation. To test this hypothesis, we analyzed DCs deficient for Asc, the key adaptor protein required for inflammasome assembly and signaling (41). Again, the inability to produce IFNI in response to polyI:C and DMXAA was maintained in Asc null, TCM-conditioned DCs (Fig. 4C and Supplementary Fig. S2C). We conclude that neither sensing via MyD88 nor inflammasome activation are implicated in the acquisition of refractoriness to innate stimuli and loss of T cell priming in tumor conditioned DCs.

A second major proposed pathway of DC suppression is through IL10 and TGFβ, two cytokines overexpressed in the TME (8, 42, 43). We performed blocking studies adding antibodies against the IL10 receptor or neutralizing TGF-β, individually or in combination. In the presence of these antibodies, release of cytokines by control cells was enhanced, confirming their blocking activity. Nevertheless, cytokine suppression by TCM was almost entirely maintained in the presence of blocking Abs, with the exception of a slight rescue induced by anti-IL10R in response to polyI:C (Fig. 4D; Supplementary Fig. S2D). Thus, IL10 and TGF-β are not exclusive factors involved in deactivation of endosomal and cytosolic sensing by tumor factors in this model.

### Lactic acid in the TCM causes loss of DC function and priming of antitumor responses

To search for alternative pathways of suppression, we next undertook a broad approach to discriminate among protein (heat sensitive) and non-protein (heat resistant) factors. The TCM was boiled followed by precipitation to eliminate denatured proteins, yielding a protein-free medium that still contains heat resistant metabolites. DCs were incubated with intact or boiled TCM, followed by restimulation with CpG-B, polyI:C and DMXAA. As shown in Fig. 5A, the ability to secrete IL12p70 and IFNI was strongly inhibited by both intact and boiled TCM. Of note, most T-cell priming suppressive activity was maintained by the boiled TCM (Fig. 5B). Together these data suggest that a heat-resistant metabolite inhibits cytokine suppression and antigen presentation.

Recent reports showed that lactic acid is an abundant, heat-resistant, metabolite in the TME of various cancer models, including lung cancer (24). We verified the presence of lactic acid by liquid chromatography-mass spectrometry (LC-MS). Indeed, both 3LL and LG TCM contained lactate, in similar amounts before and after boiling (Supplementary Fig. S3A). A colorimetric assay to quantify the amount of lactate showed that the 3LL TCM contains 60± mmol/L of lactic acid (Supplementary Fig. S3B). To

Published OnlineFirst January 23, 2018; DOI: 10.1158/0008-5472.CAN-17-1307



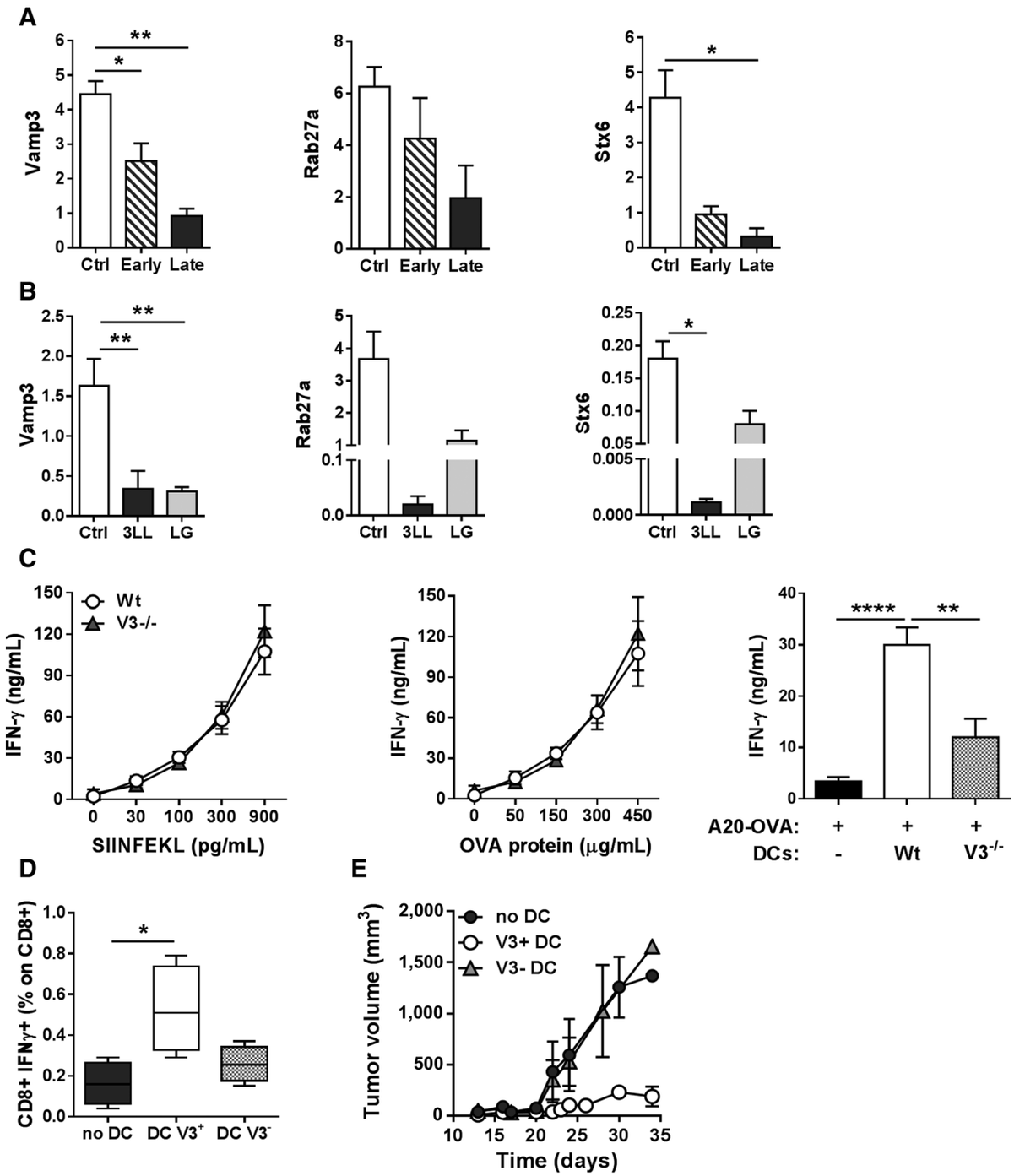


**Figure 3.**

Downregulation of VAMP3 in tumor-conditioned DCs impairs tumor rejection. **A,** qRT-PCR analysis of expression of *Vamp3, Rab27a*, and *Stx6* by lung DCs sorted from control or tumor-bearing mice at early (21 days) or late (28 days) time points. Data were normalized on Gapdh and are presented as mean ± SEM calculated from biological triplicates, each consisting of a pool of three animals. **B,** Relative expression of *Vamp3, Rab27a*, and *Stx6* by FL-DCs upon 24 hours of TCM conditioning *in vitro*. Data represent the mean± SEM of five independent experiments. **C,** *In vitro* T-cell activation induced by wt or VAMP3$^{-/-}$ FL-DCs pulsed with class I OVA peptide (left), OVA protein (middle), or apoptotic A20-OVA (right). IFNγ production was quantified by ELISA 48 hours after coincubation. Data represent the mean ± SEM of three independent experiments. **D** and **E,** 3LL-OVA were injected subcutaneously along with $3 \times 10^5$ wt or VAMP3$^{-/-}$ DCs. **D,** T-cell response was evaluated 14 days after tumor injection on total splenocytes *ex vivo* restimulated with class I OVA peptide. IFNγ production was assessed by intracellular staining and expressed as the percentage of IFNγ$^+$/CD8$^+$ T cells. Data are representative of two independent experiments with five mice per group. **E,** Tumor growth is presented as average tumor volume ± SEM. Significances have been determined by one-way ANOVA or Kruskal–Wallis test, depending on sample distribution; *, $P \leq 0.05$; **, $P \leq 0.01$; ****, $P \leq 0.0001$.

Published OnlineFirst January 23, 2018; DOI: 10.1158/0008-5472.CAN-17-1307



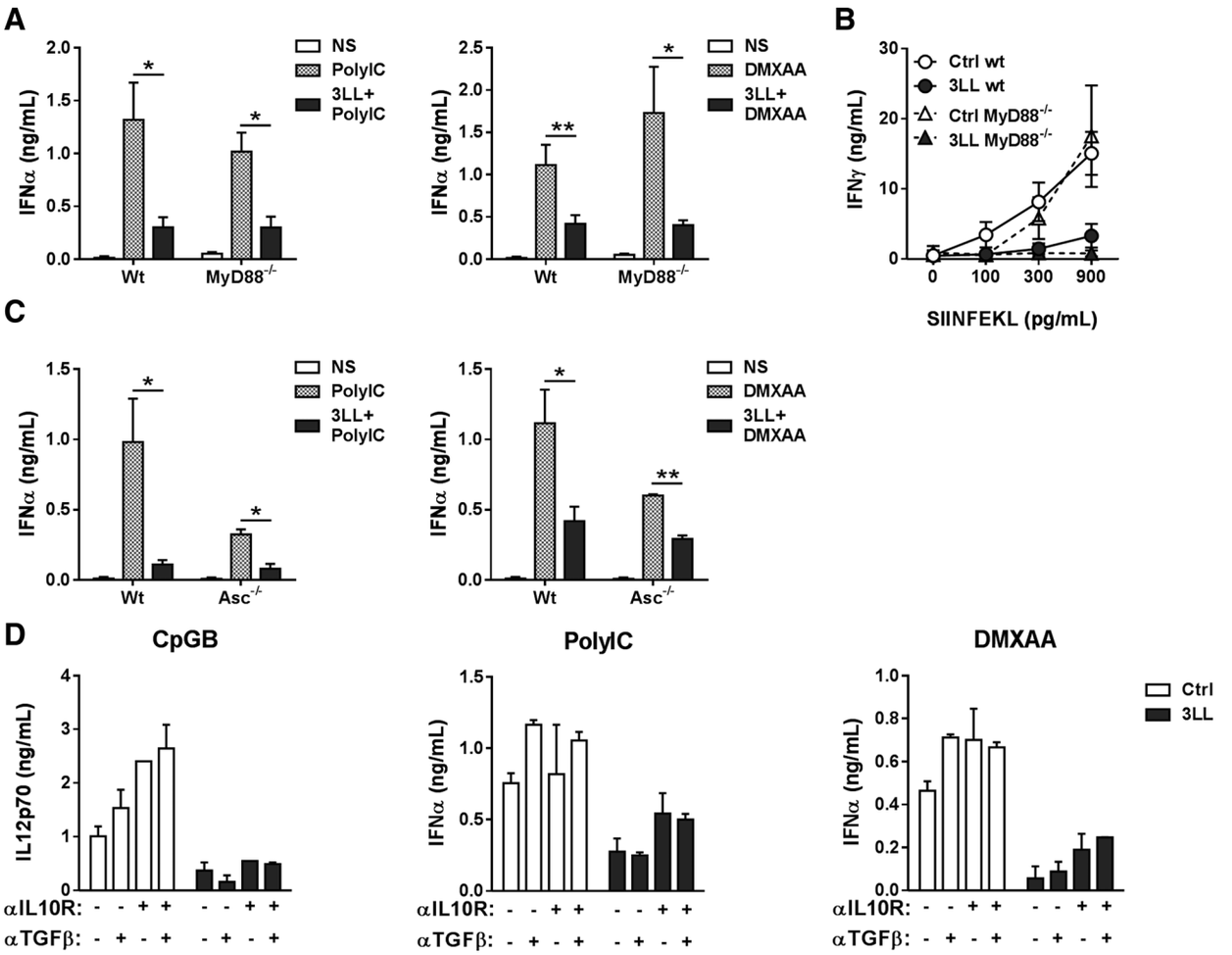


**Figure 4.**

TCM-induced DC suppression is not caused by innate sensors or anti-inflammatory cytokines. **A** and **C,** Wt, MyD88$^{-/-}$, or Asc$^{-/-}$ FL-DCs were conditioned for 24 hours with 3LL TCM, washed, and then stimulated overnight with polyI:C (10 μg/mL) or DMXAA (25 μg/mL). IFNα production was measured by ELISA. Data are presented as mean ± SEM of two independent experiments. **B,** *In vitro* T-cell activation assays. After 2 hours of conditioning with 3LL TCM (1:2), wt and MyD88$^{-/-}$ FL-DCs were pulsed with OVA class I peptide for 3 hours. DCs were then coincubated 48 hours with OT-I T cells and IFNγ production was quantified by ELISA. Data represent the mean ± SEM of two independent experiments. **D,** FL-DCs were conditioned 24 hours with 3LL TCM in the presence of αIL10R (10 μg/mL) or αTGFβ (10 μg/mL) or both, as indicated. After treatment, cells were washed and stimulated overnight with CpG-B (1 μg/mL), polyI:C (10 μg/mL), or DMXAA (25 μg/mL). IFNα and IL12p70 were measured by ELISA. Data represent mean ± SEM of one experiment out of two. Significance was determined by an unpaired *t* test. *, $P \leq 0.05$; **, $P \leq 0.01$. NS, not stimulated.

test the effect of lactate directly on DCs, we used a lower dose (10 mmol/L), to exclude any effect on viability (Supplementary Fig. S3C). Twenty-four hours conditioning with 10 mmol/L of lactic acid did not induce phenotypic maturation (Supplementary Fig. S3D), but blocked IL12p70 production after CpG-B stimulation and IFNα upon CpG-B, polyI:C and DMXAA, indicating inhibition of innate functions (Fig. 5C). To evaluate the effect of lactic acid on adaptive DCs functions control or lactate conditioned DCs were loaded with OVA class-I peptide, intact OVA protein or UV-treated apoptotic A20-OVA. As shown in Fig. 5D, lactate did not affect presentation of control peptide whereas cross-presentation of soluble OVA and cell-associated OVA was significantly inhibited, in a dose-dependent manner (Supplementary Fig. S3F).

We next used different approaches to directly prove that lactic acid in the TME is the critical metabolite responsible for DC blockade. First, as lactate was shown to partition into a low molecular weight fraction (24), we separated the TCM by size (>3 KDa and <3 KDa fractions) and confirmed that the vast majority of lactate was in the <3 KDa (Fig. 6A). When the different fractions were tested on DCs, we observed that high MW factors were significantly less suppressive than low MW factors (Fig. 6B and C). Second, we cultured lung tumor cells in the presence of an LDHA inhibitor to decrease lactate concentration in the TME (Fig. 6D). Notably, a modest reduction in lactate content resulted in a slight recovery in terms of cytokine production and T-cell activation, demonstrating a causal link between lactate content and extent of suppression (Fig. 6E and F).

To explore the mechanisms of lactate-induced block in antigen presentation, we tested intracellular pH, as this was recently shown to decrease in T cells exposed to high lactate concentration (44). DCs were incubated with pHrodo green dextran, a pH-

Published OnlineFirst January 23, 2018; DOI: 10.1158/0008-5472.CAN-17-1307



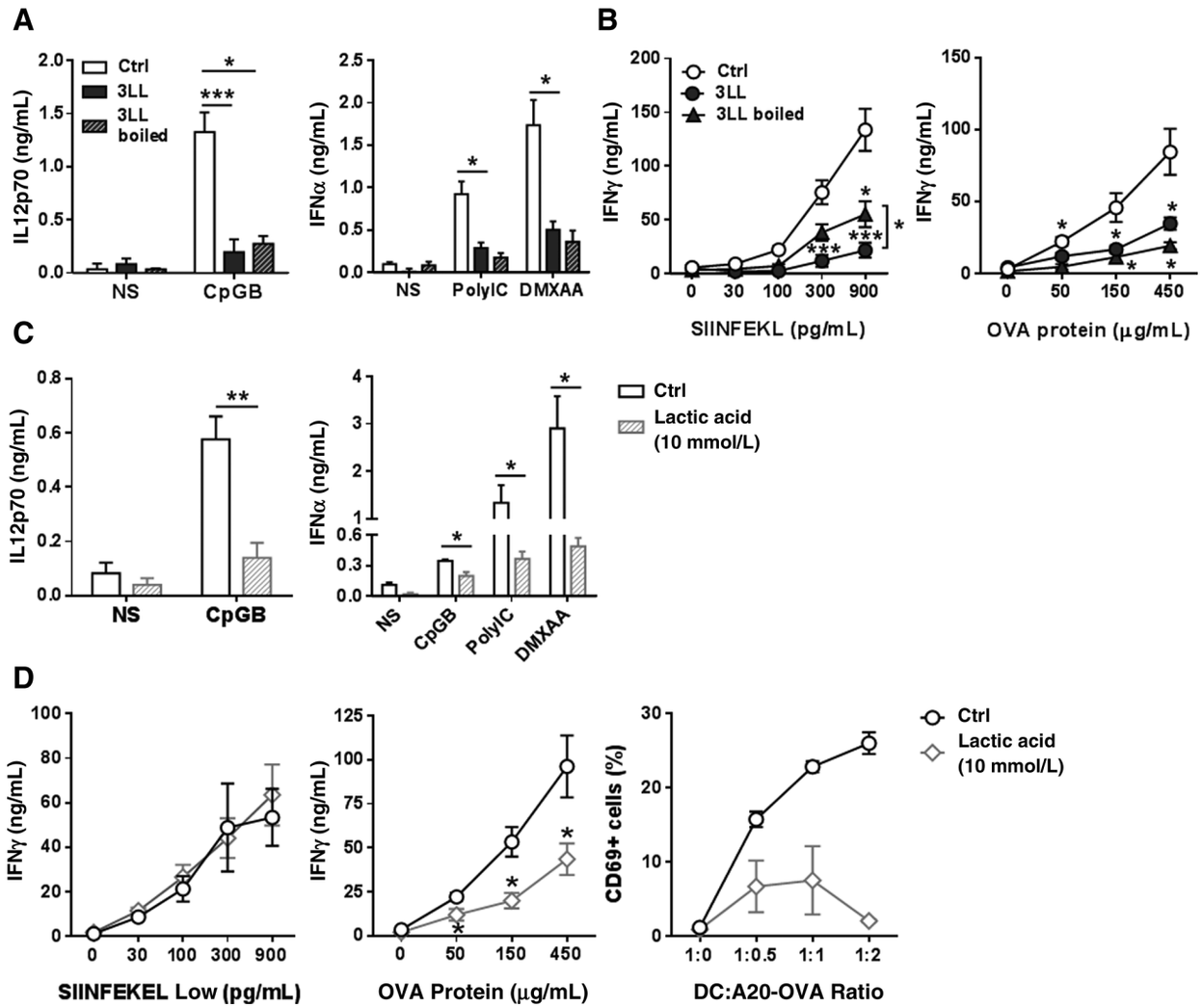


**Figure 5.**

Lactic acid inhibits innate functions and cross-presentation in DCs. **A,** DCs were conditioned with untreated 3LL TCM or boiled 3LL TCM (10′ at 95°C) for 24 hours, then washed and stimulated overnight with the indicated agonists. Cytokine production was measured by ELISA. Data represent the mean ± SEM of two or three independent experiments. **B,** 3LL- or 3LL boiled-conditioned DCs were pulsed with class I OVA antigen or OVA protein and coincubated 48 hours with OT-I T cells. Data show ELISA values of IFNγ in wells upon 48 hours of coculture. Data are mean ± SEM of two or three independent experiments. **C,** Control DCs or DCs conditioned with lactic acid (10 mmol/L) were stimulated overnight with CpG-B (1 μg/mL), DMXAA (25 μg/mL), or polyI:C (10 μg/mL). IL12p70 and IFNα production was measured by ELISA. Data represent the mean ± SEM of three or five independent experiments. **D,** Control or lactic acid-conditioned DCs were pulsed with OVA class I peptide (left), OVA protein (middle), or apoptotic A20-OVA cells (right) and coincubated with OT-I T lymphocytes. IFNγ was measured by ELISA after 48 hours of culture and percentage of $CD69^+$ cells was analyzed by FACS after 16 hours of coculture. Data represent mean ± SEM of three independent experiments. Significance was determined by an unpaired *t* test; *, $P \leq 0.05$; **, $P \leq 0.01$; ***, $P \leq 0.001$. NS, not stimulated.

sensitive probe that is internalized by endocytosis and emits fluorescence only in acidic organelles. Exposure of DCs to lactate caused a significantly higher increase in fluorescence emission as compared to ctrl cells, indicating lower endosomal pH (Fig. 6G, Supplementary Table S2). To test whether low endosomal pH may interfere with antigen degradation, we incubated control- or lactate-treated DCs with a model antigen coupled to a self-quenched conjugate that emits bright fluorescence only upon proteolytic cleavage in endosomes (DQ-BSA). Indeed, fluorescence was higher in lactate conditioned DCs in a dose-dependent way, indicating an accelerated proteolytic cleavage (Fig. 6H, Supplementary Table S3). Together these results strongly suggest that lactic acid reprogram both innate responses and antigen handling in DCs.

### Lactate inhibits DC-mediated T-cell priming and tumor rejection

Because lactic acid acted as potent suppressor of DCs functions *in vitro*, we evaluated its impact on the ability to prime antitumor responses *in vivo*. To this goal, we adoptively transferred OT-I T cells in recipient mice followed by immunization with control or lactate conditioned OVA pulsed DCs. Tissues were harvested at

Published OnlineFirst January 23, 2018; DOI: 10.1158/0008-5472.CAN-17-1307



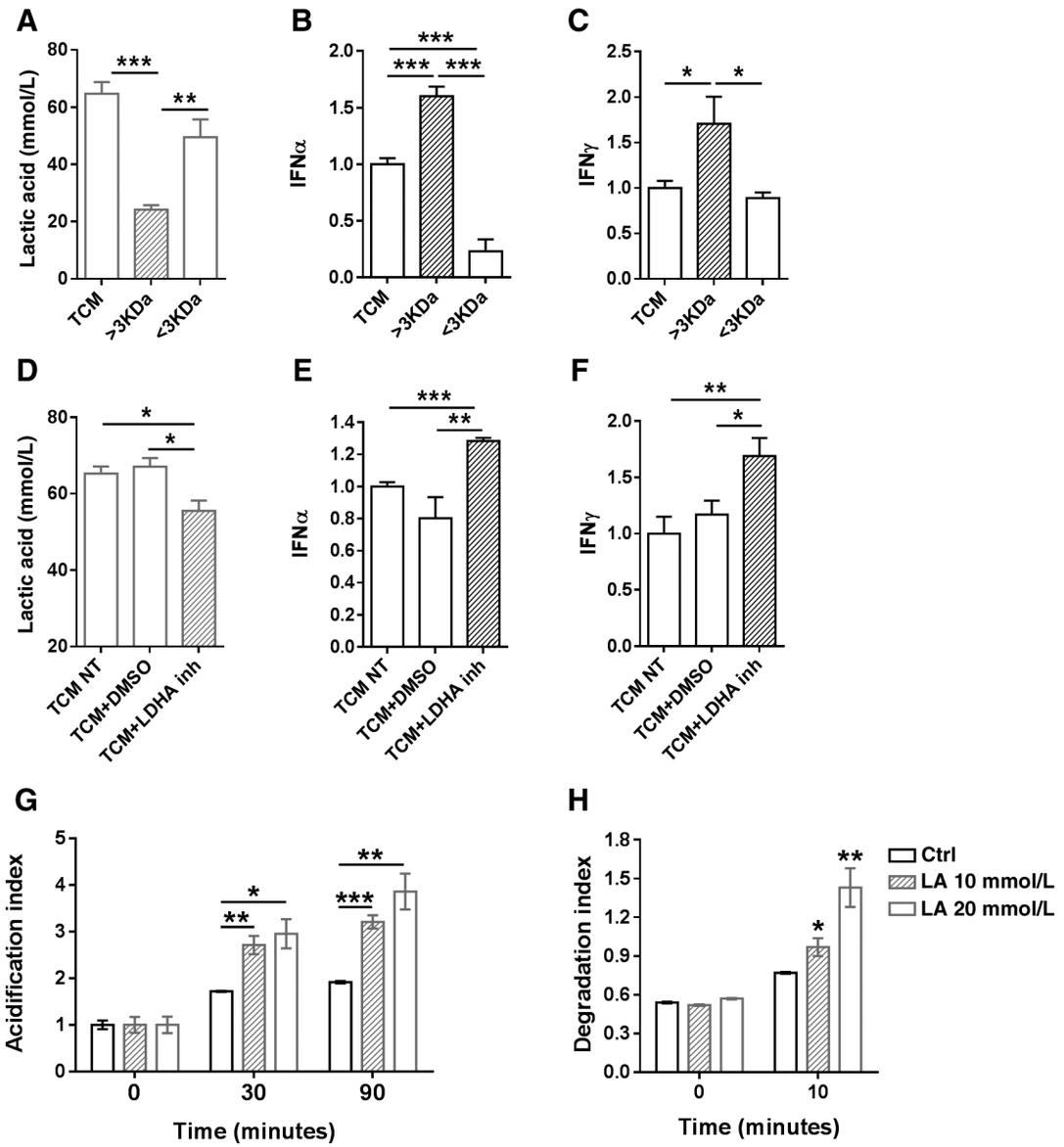


**Figure 6.**

High concentrations of lactic acid in the TME block DC functions by modifying intracellular pH. **A–C,** The TCM was size-fractionated into >3 KDa and <3 KDa fractions and used to condition DCs. **A,** Concentrations of lactic acid in the different fractions assessed by a colorimetric assay. IFNα production (**B**) and T-cell activation (**C**) by DCs conditioned with TCM fractions. **D–F,** DCs were conditioned with cell culture supernatants of tumor cells (3LL) grown in the presence of LDHA inhibitor (GSK 2837808A) or vehicle (DMSO). **D,** Lactic acid concentration in the obtained supernatants. **E,** Conditioned DCs were stimulated with CpG-B (1 μg/mL) and IFNα levels were evaluated by ELISA or pulsed with OVA protein (300 μg/mL) and mixed with T cells, and IFNγ was evaluated by ELISA after 48 hours of culture (**F**). Data are presented as mean ± SEM of fold induction on TCM of three independent experiments. **G,** Control or LA-DCs (10 or 20 mmol/L) were pulsed with pH-sensitive pHrodo Green dye 15′ at 37°C. Cells were then washed and blocked at 4°C (t0) or incubated 30′ and 90′ at 37°C to allow internalization. Data are presented as acidification index that represent mean ± SEM of pH-rodo Green MFI, normalized on t0 of three independent experiments. **H,** Control DCs or LA-DCs (10 or 20 mmol/L) were pulsed with DQ-BSA and A647-BSA (as control of uptake) 15′ at 37°C. Cells were then washed and fixed (t0) or incubated 10′ at 37°C (t10) to allow degradation. The percentage of FITC/DQ-BSA$^+$ cells was assessed by flow cytometry as an index of degradation. Data were normalized on the uptake of A647-OVA and represent mean ± SEM of three independent experiments. Significance was determined by unpaired *t* test; *, $P \leq 0.05$; **, $P \leq 0.01$; ***, $P \leq 0.001$. LA, lactic acid.

day 15 post-priming to analyze the presence of IFNγ producing effector T cells. Injection of wt DCs expanded a population of OVA-specific effector CD8$^+$ T cells that was significantly reduced in mice immunized with lactate conditioned DCs (Fig. 7A and B). Finally, animals immunized with control or lactate-treated DCs were inoculated with 3LL-OVA cells subcutaneously. Immunization with control DCs strongly reduced tumor volume and tumor engraftment (40% as compared to 100% in no DCs group) and significantly prolonged survival. In contrast, lactate-treated DCs were significantly less efficient in conferring

Published OnlineFirst January 23, 2018; DOI: 10.1158/0008-5472.CAN-17-1307



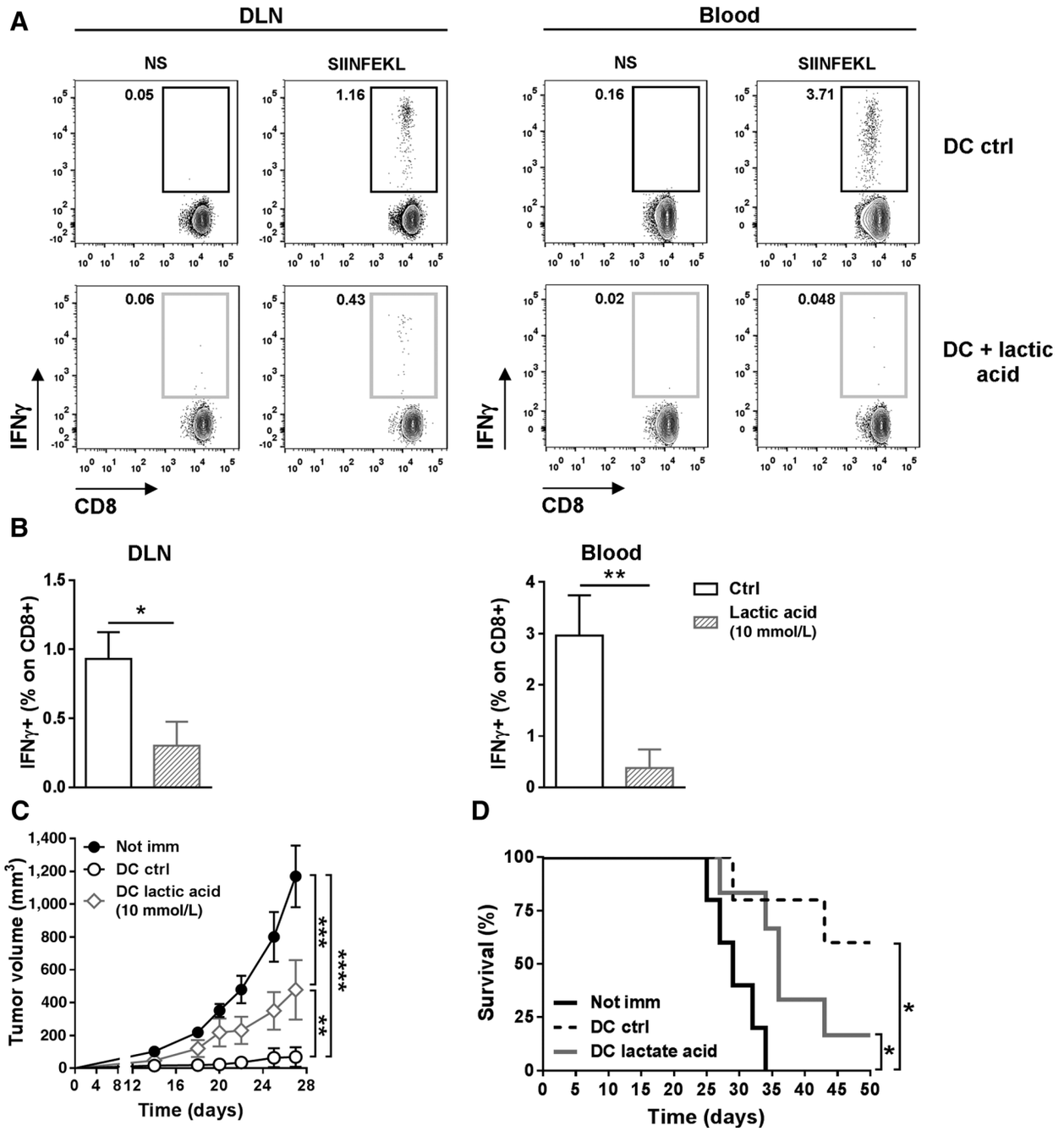


**Figure 7.**

Lactic acid constrains DC-induced priming of antitumoral T-cell response. **A** and **B,** *In vivo* T-cell priming. Control or lactic acid–conditioned DCs were stimulated with CpG-B (1 μg/mL) and polyI:C (1 μg/mL) and pulsed with class I OVA peptide for 3 hours. Cells were then washed and injected in the footpad of C57BL/6 mice, previously transferred with RagOT-I intravenously 14 days after DCs injection; blood and popliteal lymph nodes were collected and restimulated *ex vivo* with class I OVA peptide. IFNγ production was measured by intracellular staining and flow cytometry analysis. Representative dot-plots (**A**) and percentages (**B**) of IFNγ$^+$ CD8 T cells are shown. Data represent the mean ± SEM of two independent experiments. Significance was determined by unpaired *t* test; *, $P \leq 0.05$; **, $P \leq 0.01$. NS, not stimulated. **C** and **D,** 3LL-OVA cells ($3 \times 10^5$ cells/mice) were injected subcutaneously in the right flank of mice 14 days after *in vivo* T-cell priming induced by subcutaneous injection of control or LA-DCs. Data are presented as tumor growth profile (left) and as the percentage of survival (right). Tumor growth profiles were compared using two-way ANOVA and tumor survival by log-rank (Mantel-Cox) test; **, $P \leq 0.01$; ***, $P \leq 0.001$; ****, $P \leq 0.0001$.

protection from tumor challenge, in terms of tumor volume, engraftment (83% of mice developed tumors) and animal survival (Fig. 7C and D).

In conclusion, the data show that lactic acid contained in the TME has a potent immune-suppressive action on DCs abrogating priming of antitumoral responses *in vivo*.

Published OnlineFirst January 23, 2018; DOI: 10.1158/0008-5472.CAN-17-1307



## Discussion

Development of combinatorial therapies to target multiple immune breaks in the microenvironment is a promising future approach in cancer. Of the various pathways that conspire to inhibit activation of cytotoxic T lymphocytes, loss of antigen presentation in the proper stimulatory context is still a poorly understood process. Here, we have undertaken an accurate analysis of the functional impairment experienced by DCs exposed to lung cancer tumor-derived factors. We compared *bona fide* DCs isolated from lung tissues implanted orthotopically with 3LL cells and their equivalent isolated from healthy lungs. The isolated population excludes $CD11c^+$ alveolar macrophages and includes the two subsets of conventional DCs CD103 and CD11b DCs, specialized in antigen cross-presentation and cytokine production, respectively (45). Our data show that these subset-specific functions, analyzed in bulk, are both targeted when the lung is infiltrated by a tumor. In parallel, we exposed DCs to medium conditioned by a whole-tumor extract, that includes cancer cells and their surrounding stroma. Using both approaches and measuring independently cytokine production and T-cell priming, we found that conditioning blocks the ability to secrete IL12 and type-I interferon in response to agonist of TLR9, TLR3, and STING. Inability to respond to LPS or IFNγ/CD40 was previously shown to depend on tumor derived PGE-2, IL10, or miRNA reprogramming (3, 8, 46, 47). Our data extend the concept of innate suppression showing that tumor-exposed DCs become refractory to stimulation by agonist of TLR3 and STING and, importantly, become unable to secrete IFNI. Type-I interferon in DCs is critical for immunosurveillance of nascent tumors, cross-priming and tumor rejection (7, 48, 49). In established tumors, however, plasmacytoid DCs were shown to silence IFNI production, suggesting the existence of an escape mechanism that targets the IFN axis (50). Our data show that also conventional DCs lose the ability to respond to exogenous nucleic acids, indicating that crippling cytosolic sensing and the ensuing IFNI in cross-presenting DCs may be a further mechanism to avoid T-cell recognition.

Innate immune memory is emerging as a key feature of myeloid cells that, depending on the type and concentration of ligand encountered, respond with enhanced or decreased cytokine production upon restimulation (51). Maturation and early cytokine induction upon TCM exposure suggest triggering of innate sensors by soluble factors, which in turn may induce tolerance to further stimulation. A search for innate sensing pathways engaged by soluble factors in the TCM excluded a role for MyD88, Asc. A reasonable hypothesis is that multiple pathways act in concert when DCs encounter complex signals such as those contained in the TME, making analysis of individual component poorly informative. Our observation of a broad refractoriness to a variety of different stimuli and the inability to produce both NF-kB and IRF-dependent cytokines support the possibility of epigenetic remodeling to explain cytokine loss.

A second interesting finding is that proteins involved in the control of intracellular trafficking pathways are transcriptionally down in tumor-exposed DCs. A similar strategy of immune evasion is put in place during CMV infection when multiple genes of the host secretory pathways are targeted by virus-induced miRNA expression (35). Indeed, several miRNAs were implicated in suppressing antigen-presenting functions in DCs exposed to lung cancer factors (46, 47), which might interfere with expression of membrane trafficking modules. Our findings provide an example of the impact of interfering with trafficking proteins as in the case of VAMP3 that controls the dynamic fusion of recycling endosomes to phagosomes and transport of H-ATPase, two critical steps in cross-presentation (32, 52, 53).

Third, using a top-down approach, we identified lactic acid as crucial soluble component of the TME that affects DCs functioning. Lactic acid recapitulates most of the suppressive effects induced by the whole TCM and a minor reduction in its amount is reflected into a corresponding functional rescue. On these bases, we concluded that lactate is a key inhibitory small metabolite that likely operates in combination with others soluble factors, whose specific activities remain to be determined. Earlier reports had indicated an effect of lactic acid on DCs (22, 26, 54). The strong inhibition of type-I interferon in response to CpGB, polyI:C and STING agonist, induced by lactate is not simply due to desensitization, as lactic acid does not induce DCs maturation. Metabolic changes induced by a block in glycolysis in the presence of high lactate concentration may underlie the incapacity to support cytokine production. In addition, lactic acid exerts a selective action on DC by accelerating antigens degradation that, according to established models, impairs preservation of epitopes for MHC class-I loading in phagosomes. As SNAREs were not modulated by lactic acid (Supplementary Fig. S3E), the data indicate the coexistence of multiple independent ways to avoid class-I presentation in the TME. Importantly, concomitant suppression of innate and adaptive functions by lactate cooperates to ablate T-cell priming and tumor rejection *in vivo*.

In conclusion, our study highlights multilevel overlapping mechanisms that independently target cytokine responses and antigen processing whose combination cooperates to disable DCs functions in the TME.

### Disclosure of Potential Conflicts of Interest

No potential conflicts of interest were disclosed.

### Authors' Contributions

**Conception and design:** N. Caronni, F. Benvenuti
**Development of methodology:** N. Caronni, F. Simoncello, F. Stafetta
**Acquisition of data (provided animals, acquired and managed patients, provided facilities, etc.):** N. Caronni, F. Simoncello, F. Stafetta, C. Guarnaccia, J.S. Ruiz-Moreno, B. Opitz, T. Galli, V. Proux-Gillardeaux
**Analysis and interpretation of data (e.g., statistical analysis, biostatistics, computational analysis):** N. Caronni, F. Simoncello, C. Guarnaccia
**Writing, review, and/or revision of the manuscript:** N. Caronni, T. Galli, V. Proux-Gillardeaux, F. Benvenuti
**Study supervision:** F. Benvenuti

### Acknowledgments

This work was supported by grant IG2013 14414 from the Italian Association for Cancer Research (AIRC; to F. Benvenuti) and grant 14-0320 from Worldwide Cancer Research (WWCR; to F. Benvenuti). We are grateful to Vasilena Gocheva and members of the Tyler Jacks's laboratory for providing the LG tumor cell line and to D. Fearon for providing LLC/1 tumor cell line transduced with OVA (3LL-OVA) cells. We thank V.M. Dixit (Genetech) for $Asc^{-/-}$ mice and Cecilia Garlanda for shipping $MyD88^{-/-}$ bone marrow.

The costs of publication of this article were defrayed in part by the payment of page charges. This article must therefore be hereby marked *advertisement* in accordance with 18 U.S.C. Section 1734 solely to indicate this fact.

Received May 4, 2017; revised October 13, 2017; accepted January 18, 2018; published OnlineFirst January 23, 2018.

## References


1. Pfirschke C, Engblom C, Rickelt S, Cortez-Retamozo V, Garris C, Pucci F, et al. Immunogenic chemotherapy sensitizes tumors to checkpoint blockade therapy. Immunity 2016;44:343–54.
2. Salmon H, Idoyaga J, Rahman A, Leboeuf M, Remark R, Jordan S, et al. Expansion and activation of CD103(+) dendritic cell progenitors at the tumor site enhances tumor responses to therapeutic PD-L1 and BRAF inhibition. Immunity 2016;44:924–38.
3. Zelenay S, van der Veen AG, Bottcher JP, Snelgrove KJ, Rogers N, Acton SE, et al. Cyclooxygenase-dependent tumor growth through evasion of immunity. Cell 2015;162:1257–70.
4. Broz ML, Binnewies M, Boldajipour B, Nelson AE, Pollack JL, Erle DJ, et al. Dissecting the tumor myeloid compartment reveals rare activating antigen-presenting cells critical for T cell immunity. Cancer Cell 2014;26:638–52.
5. Ma Y, Adjemian S, Mattarollo SR, Yamazaki T, Aymeric L, Yang H, et al. Anticancer chemotherapy-induced intratumoral recruitment and differentiation of antigen-presenting cells. Immunity 2013;38:729–41.
6. Garg AD, Galluzzi L, Apetoh L, Baert T, Birge RB, Bravo-San Pedro JM, et al. Molecular and translational classifications of DAMPs in immunogenic cell death. Front Immunol 2015;6:588.
7. Woo SR, Fuertes MB, Corrales L, Spranger S, Furdyna MJ, Leung MY, et al. STING-dependent cytosolic DNA sensing mediates innate immune recognition of immunogenic tumors. Immunity 2014;41:830–42.
8. Ruffell B, Chang-Strachan D, Chan V, Rosenbusch A, Ho CM, Pryer N, et al. Macrophage IL-10 blocks CD8+ T cell-dependent responses to chemotherapy by suppressing IL-12 expression in intratumoral dendritic cells. Cancer Cell 2014;26:623–37.
9. Marigo I, Zilio S, Desantis G, Mlecnik B, Agnellini AH, Ugel S, et al. T cell cancer therapy requires CD40-CD40L activation of tumor necrosis factor and inducible nitric-oxide-synthase-producing dendritic cells. Cancer Cell 2016;30:651.
10. Laoui D, Keirsse J, Morias Y, Van Overmeire E, Geeraerts X, Elkrim Y, et al. The tumour microenvironment harbours ontogenically distinct dendritic cell populations with opposing effects on tumour immunity. Nat Commun 2016;7:13720.
11. Ma Y, Shurin GV, Peiyuan Z, Shurin MR. Dendritic cells in the cancer microenvironment. J Cancer 2013;4:36–44.
12. Veglia F, Gabrilovich DI. Dendritic cells in cancer: the role revisited. Curr Opin Immunol 2017;45:43–51.
13. Cubillos-Ruiz JR, Silberman PC, Rutkowski MR, Chopra S, Perales-Puchalt A, Song M, et al. ER stress sensor XBP1 controls anti-tumor immunity by disrupting dendritic cell homeostasis. Cell 2015;161:1527–38.
14. Herber DL, Cao W, Nefedova Y, Novitskiy SV, Nagaraj S, Tyurin VA, et al. Lipid accumulation and dendritic cell dysfunction in cancer. Nat Med 2010;16:880–6.
15. Joffre OP, Segura E, Savina A, Amigorena S. Cross-presentation by dendritic cells. Nat Rev Immunol 2012;12:557–69.
16. Chiaruttini G, Piperno GM, Jouve M, De Nardi F, Larghi P, Peden AA, et al. The SNARE VAMP7 regulates exocytic trafficking of interleukin-12 in dendritic cells. Cell Rep 2016;14:2624–36.
17. Proux-Gillardeaux V, Rudge R, Galli T. The tetanus neurotoxin-sensitive and insensitive routes to and from the plasma membrane: fast and slow pathways? Traffic 2005;6:366–73.
18. Das V, Nal B, Dujeancourt A, Thoulouze MI, Galli T, Roux P, et al. Activation-induced polarized recycling targets T cell antigen receptors to the immunological synapse; involvement of SNARE complexes. Immunity 2004;20:577–88.
19. Murray RZ, Kay JG, Sangermani DG, Stow JL. A role for the phagosome in cytokine secretion. Science 2005;310:1492–5.
20. Fantin VR, St-Pierre J, Leder P. Attenuation of LDH-A expression uncovers a link between glycolysis, mitochondrial physiology, and tumor maintenance. Cancer Cell 2006;9:425–34.
21. Girgis H, Masui O, White NM, Scorilas A, Rotondo F, Seivwright A, et al. Lactate dehydrogenase A is a potential prognostic marker in clear cell renal cell carcinoma. Mol Cancer 2014;13:101.
22. Dietl K, Renner K, Dettmer K, Timischl B, Eberhart K, Dorn C, et al. Lactic acid and acidification inhibit TNF secretion and glycolysis of human monocytes. J Immunol 2010;184:1200–9.
23. Husain Z, Huang Y, Seth P, Sukhatme VP. Tumor-derived lactate modifies antitumor immune response: effect on myeloid-derived suppressor cells and NK cells. J Immunol 2013;191:1486–95.
24. Colegio OR, Chu NQ, Szabo AL, Chu T, Rhebergen AM, Jairam V, et al. Functional polarization of tumour-associated macrophages by tumour-derived lactic acid. Nature 2014;513:559–63.
25. Brand NR, Opoka RO, Hamre KE, John CC. Differing causes of lactic acidosis and deep breathing in cerebral malaria and severe malarial anemia may explain differences in acidosis-related mortality. PLoS ONE 2016;11:e0163728.
26. Gottfried E, Kunz-Schughart LA, Ebner S, Mueller-Klieser W, Hoves S, Andreesen R, et al. Tumor-derived lactic acid modulates dendritic cell activation and antigen expression. Blood 2006;107:2013–21.
27. Adachi O, Kawai T, Takeda K, Matsumoto M, Tsutsui H, Sakagami M, et al. Targeted disruption of the MyD88 gene results in loss of IL-1- and IL-18-mediated function. Immunity 1998;9:143–50.
28. DuPage M, Cheung AF, Mazumdar C, Winslow MM, Bronson R, Schmidt LM, et al. Endogenous T cell responses to antigens expressed in lung adenocarcinomas delay malignant tumor progression. Cancer Cell 2011;19:72–85.
29. Dimitrova N, Gocheva V, Bhutkar A, Resnick R, Jong RM, Miller KM, et al. Stromal expression of miR-143/145 promotes neoangiogenesis in lung cancer development. Cancer Discov 2016;6:188–201.
30. Benvenuti F, Hugues S, Walmsley M, Ruf S, Fetler L, Popoff M, et al. Requirement of Rac1 and Rac2 expression by mature dendritic cells for T cell priming. Science 2004;305:1150–3.
31. Day PM, Yewdell JW, Porgador A, Germain RN, Bennink JR. Direct delivery of exogenous MHC class I molecule-binding oligopeptides to the endoplasmic reticulum of viable cells. PNAS 1997;94:8064–9.
32. Jancic C, Savina A, Wasmeier C, Tolmachova T, El-Benna J, Dang PM, et al. Rab27a regulates phagosomal pH and NADPH oxidase recruitment to dendritic cell phagosomes. Nat Cell Biol 2007;9:367–78.
33. Cebrian I, Visentin G, Blanchard N, Jouve M, Bobard A, Moita C, et al. Sec22b regulates phagosomal maturation and antigen crosspresentation by dendritic cells. Cell 2011;147:1355–68.
34. Reefman E, Kay JG, Wood SM, Offenhauser C, Brown DL, Roy S, et al. Cytokine secretion is distinct from secretion of cytotoxic granules in NK cells. J Immunol 2010;184:4852–62.
35. Hook L, Hancock M, Landais I, Grabski R, Britt W, Nelson JA. Cytomegalovirus microRNAs. Curr Opin Virol 2014;7:40–6.
36. Bartee E, McCormack A, Fruh K. Quantitative membrane proteomics reveals new cellular targets of viral immune modulators. PLoS Pathog 2006;2:e107.
37. Galli T, Chilcote T, Mundigl O, Binz T, Niemann H, De Camilli P. Tetanus toxin-mediated cleavage of cellubrevin impairs exocytosis of transferrin receptor-containing vesicles in CHO cells. J Cell Biol 1994;125:1015–24.
38. Bock JB, Klumperman J, Davanger S, Scheller RH. Syntaxin 6 functions in trans-Golgi network vesicle trafficking. Mol Biol Cell 1997;8:1261–71.
39. Yang C, Mora S, Ryder JW, Coker KJ, Hansen P, Allen LA, et al. VAMP3 null mice display normal constitutive, insulin- and exercise-regulated vesicle trafficking. Mol Cell Biol 2001;21:1573–80.
40. Tang M, Diao J, Gu H, Khatri I, Zhao J, Cattral MS. Toll-like receptor 2 activation promotes tumor dendritic cell dysfunction by regulating IL-6 and IL-10 receptor signaling. Cell Rep 2015;13:2851–64.
41. Martinon F, Burns K, Tschopp J. The inflammasome: a molecular platform triggering activation of inflammatory caspases and processing of proIL-beta. Mol Cell 2002;10:417–26.
42. Ghiringhelli F, Puig PE, Roux S, Parcellier A, Schmitt E, Solary E, et al. Tumor cells convert immature myeloid dendritic cells into TGF-beta-secreting cells inducing CD4+CD25+ regulatory T cell proliferation. J Exp Med 2005;202:919–29.
43. Luo X, Tarbell KV, Yang H, Pothoven K, Bailey SL, Ding R, et al. Dendritic cells with TGF-beta1 differentiate naive CD4+CD25- T cells into islet-protective Foxp3+ regulatory T cells. PNAS 2007;104:2821–6.
44. Brand A, Singer K, Koehl GE, Kolitzus M, Schoenhammer G, Thiel A, et al. LDHA-associated lactic acid production blunts tumor immunosurveillance by T and NK cells. Cell Metab 2016;24:657–71.
45. Merad M, Sathe P, Helft J, Miller J, Mortha A. The dendritic cell lineage: ontogeny and function of dendritic cells and their subsets in the steady state and the inflamed setting. Annu Rev Immunol 2013;31:563–604.
46. Pyfferoen L, Brabants E, Everaert C, De Cabooter N, Heyns K, Deswarte K, et al. The transcriptome of lung tumor-infiltrating dendritic cells reveals a

Published OnlineFirst January 23, 2018; DOI: 10.1158/0008-5472.CAN-17-1307



tumor-supporting phenotype and a microRNA signature with negative impact on clinical outcome. Oncoimmunology 2017;6:e1253655.
47. Pyfferoen L, Mestdagh P, Vergote K, De Cabooter N, Vandesompele J, Lambrecht BN, et al. Lung tumours reprogram pulmonary dendritic cell immunogenicity at the microRNA level. Int J Cancer 2014;135: 2868–77.
48. Diamond MS, Kinder M, Matsushita H, Mashayekhi M, Dunn GP, Archambault JM, et al. Type I interferon is selectively required by dendritic cells for immune rejection of tumors. J Exp Med 2011;208:1989–2003.
49. Deng L, Liang H, Xu M, Yang X, Burnette B, Arina A, et al. STING-dependent cytosolic DNA sensing promotes radiation-induced type I interferon-dependent antitumor immunity in immunogenic tumors. Immunity 2014;41:843–52.
50. Sisirak V, Faget J, Gobert M, Goutagny N, Vey N, Treilleux I, et al. Impaired IFN-alpha production by plasmacytoid dendritic cells favors regulatory T-cell expansion that may contribute to breast cancer progression. Cancer Res 2012;72:5188–97.
51. Alvarez-Errico D, Vento-Tormo R, Sieweke M, Ballestar E. Epigenetic control of myeloid cell differentiation, identity and function. Nat Rev Immunol 2015;15:7–17.
52. Nair-Gupta P, Baccarini A, Tung N, Seyffer F, Florey O, Huang Y, et al. TLR signals induce phagosomal MHC-I delivery from the endosomal recycling compartment to allow cross-presentation. Cell 2014;158:506–21.
53. Breton S, Nsumu NN, Galli T, Sabolic I, Smith PJ, Brown D. Tetanus toxin-mediated cleavage of cellubrevin inhibits proton secretion in the male reproductive tract. Am J Physiol Ren Physiol 2000;278:F717–25.
54. Hoque R, Farooq A, Ghani A, Gorelick F, Mehal WZ. Lactate reduces liver and pancreatic injury in Toll-like receptor- and inflammasome-mediated inflammation via GPR81-mediated suppression of innate immunity. Gastroenterology 2014;146:1763–74.

Published OnlineFirst January 23, 2018; DOI: 10.1158/0008-5472.CAN-17-1307

Cancer Research
The Journal of Cancer Research (1916–1930) | The American Journal of Cancer (1931–1940)

AACR American Association for Cancer Research

# Downregulation of Membrane Trafficking Proteins and Lactate Conditioning Determine Loss of Dendritic Cell Function in Lung Cancer

Nicoletta Caronni, Francesca Simoncello, Francesca Stafetta, et al.

*Cancer Res* 2018;78:1685-1699. Published OnlineFirst January 23, 2018.